ОБЪЕДИНЕННЫЙ
ИНСТИТУТ
ЯДЕРНЫХ
ИССЛЕДОВАНИЙ

Дубна

E4-96-478

R.A.Eramzhyan[1], V.A.Kuz'min, T.V.Tetereva[2]

CALCULATIONS OF THE ORDINARY AND RADIATIVE MUON CAPTURE ON ^{58,60,62}Ni

Submitted to «Nuclear Physics A»

[1]Institute of Nuclear Research, RAS, Moscow, Russia
[2]Skobeltsyn Nuclear Physics Institute, Moscow State University, Moscow, Russia

1996

Introduction

Investigations of the Ordinary (OMC) and Radiative muon capture (RMC) are carried out over several decades. This activity achieved maximum at sixties-seventies, when the main regularities of elementary processes were elucidated and the basic mechanism of muon capture by complex nuclei was established. After that over a long time there was a pause in the experiment after which the interest in muon capture was reborn. But at present much attention is paid to the RMC. Already at the early stage of muon capture studies it was recognized that despite the fact that the radiation branching ratio is small (by four orders of magnitude compared to OMC), the effect of the pseudoscalar coupling near the pole in the pion propagator, i.e., near the high-energy tail of the photon spectrum is enhanced. The magnitude of this coupling until present was determined with a low accuracy though that many efforts were undertaken to do it with a high precision.

Interest in RMC was rekindled first of all due to a great progress in the experimental technique. This progress made it possible to measure the energy of outgoing hard photons with a high precision. The second attractive point for extensive experimental study of RMC is the existing predictions of week sensitivity of its observables to nuclear structure, especially, if they are calculated with respect to OMC. And finally, contrary to OMC, where only a single inclusive observable can be measured (besides the partial transitions in light nuclei) in RMC the spectrum of hard γ-quanta is measured. This spectrum is connected with the excitation spectrum of nuclei.

The progress in the theory demonstrated that the nuclear structure is not so passive in the muon capture. However, to take account of all details of this structure is a very complicated task since the RMC amplitudes should be summed over all possible final states. These final states form the spin-flip giant resonances in charge-exchange channels. In the medium nuclei, the contribution comes from the $L = 0$, 1 and 2 multipolarities. In heavy nuclei some contribution from the higher multipolarities is noticeable.

During the last years the huge work was done on the experimental investigation of the charge-exchange channel in neutron-proton reactions. The resonances excited in this reaction are the same as the ones which form the nuclear response in the RMC. The essential advantage of (n,p) reaction is the possibility to experimentally separate the contributions of different multipoles, which cannot be done in the RMC reaction. But on the other hand, the contribution of multi-step processes to RMC appear to be considerably less than that to the (n,p) reaction in which they bring a noticeable uncertainty in the extracted strength of the transitions into different energy regions.

For this reason it is important to discuss the processes under consideration in the framework of the same approach to the nuclear structure in order to have a possibility to estimate the quality of the solution of the nuclear part of the problem. Only afterward one can ask the question about modification of the induced pseudoscalar coupling constant inside the nuclear media. It should be mentioned that all previous calculations of RMC on medium nuclei used the nuclear models which cannot treat the unified problem of description of the set of processes leading to the same nuclear final states.

The present paper is the first attempt to combine the quasiparticle random phase approximation (QRPA) for the description of the nuclear excitation function with the OMC and RMC reaction mechanisms. The $^{58,60,62}Ni$ isotopes were chosen for the discussion because (i) the experimental measurements of RMC are carried on; (ii) there are rather complete experimental data on (n,p) and (p,n) reactions on these nuclei; (iii) simultaneous investigation of three isotopes in the same approach allows one to reveal the influence of the neutron subshells filling on the gross-structure of the charge-exchange resonances.

The paper is organized in the following way. The second section contains a sketch of the approximations and formulae used for the calculations of the RMC and OMC rates on nuclei. The third section is devoted to the solution of nuclear part of the problem. It consists of short description of the nuclear model Hamiltonian, the review of the QRPA approach to its diagonalization. The description of strength

functions of isovector spin-multipole transitions on the base of QRPA and comparison of them with the strength functions extracted from the charge-exchange direct reactions allow us to fix the parameters of effective nuclear residual interactions. The obtained excitation energies and transition amplitudes of certain operators are used for calculations of the OMC and RMC rates. The results of calculations of the total OMC rates for few values of g_P are presented in the fourth section. They are compared with the results of other authors and with the experimental data. The fifth section contains the results of calculations of the spectra of hard photons emitted under RMC and total RMC rates. The main results of the paper are summarized in the conclusion.

OMC and RMC rates

The experimentally observable quantity in RMC is the photon spectrum. We calculate it by summing the partial spectra over the nuclear final states:

$$\Lambda(k) = \sum_f \Lambda_{fi}(k)\,.$$

The photon yield $\Lambda_{fi}(k)$ corresponding to the transition from the ground state $|J_i>$ to the state $|J_f>$ is given as

$$\begin{aligned}\Lambda_{fi} &= \frac{(\alpha Z)^3}{(2\pi)^4}\alpha(G\cos\theta_C)^2 m_\mu R(Z) k(k_{fi}^{max}-k)^2 \times \\ &\times\frac{1}{2J_i+1}\sum_{\lambda M_i M_f} M^\dagger(\lambda;fi)M(\lambda;fi)\,,\end{aligned}$$

where $\vec{k} = k\hat{\vec{k}}$ is the momentum and λ is the polarisation index of the photon; α and G is the electromagnetic and weak coupling constants, respectively; θ_C is the Cabbibo angle and $R(Z)$ is the average value of muon density over the nucleus volume [2]. The maximum photon energy is given by $k^{max} = m_\mu - e_\mu - (E_f - E_i)$, where M_μ (e_μ) is the muon mass (binding energy, calculated by approximations of [4]), $E_f - E_i$ is the nuclear excitation energy. All excitation energies are reckoned from the ground state of parent nucleus.

The nuclear RMC amplitude $M(\lambda; fi)$ is described in detail in [3]. Here we have to say that in [3] two ways of RMC calculations are discussed. One way — to use the elementary amplitude of [1] for calculating all partial transition rates and then to sum up them. It is a usual impulse approximation (IA). The second way just suggested in [3] consists in modification of the IA. According to their suggestion one should use the continuity equation for the electromagnetic current together with the $SU(2) \times SU(2)$ current-algebra commutator. This procedure takes into account many-body currents like the meson-exchange ones. After this modification all partial transition are evaluated and summed up. This version is called as MIA — modified impulse approximation.

Below we present the results of calculations performed in both approximations.

Usually the photon spectra $\Lambda(k)$ are normalized by the total OMC rate. That is why we have calculated the total OMC rates too. It is calculated as the sum of partial OMC rates over the final nucleus state

$$\Lambda^{OMC} = \sum_f \Lambda^{OMC}_{fi} ,$$

where

$$\Lambda^{OMC}_{fi} = \frac{(\nu G \cos\theta_C)^2}{\pi\hbar}(m_\mu \alpha Z)^3 R(Z) \times \\ \times \frac{1}{2J_i+1} \sum_{M_i, M_f} M^\dagger_{OMC}(fi) M_{OMC}(fi) .$$

Nuclear response calculation

The nuclear amplitudes to describe the OMC and RMC are calculated within the random phase approximation (RPA). For completeness we give the short description of formalism of quasiparticle random phase approximation (QRPA) which is extension of usual RPA to the non-closed shell nuclei; afterwards we will discuss how the parameters of residual interaction were fixed.

Nuclear model Hamiltonian [5] consists of the spherical single-particle potentials of Woods-Saxon shape each for neutrons and protons, a superconducting monopole pairing between like particles, and of isotopic invariant residual interaction, taken in separable form:

$$H_M = \sum_{\tau=n,p} H_0(\tau) + H_{res},$$

where

$$H_0(\tau) = \sum_{j_\tau, m_\tau} E_{j_\tau} a^\dagger_{j_\tau, m_\tau} a_{j_\tau, m_\tau} - \\ -\frac{G_\tau}{4} \sum_{j'_\tau, m'_\tau, j_\tau m_\tau} (-)^{j'_\tau - m'_\tau + j_\tau - m_\tau} a^\dagger_{j'_\tau, m'_\tau} a^\dagger_{j'_\tau, -m'_\tau} a_{j_\tau, -m_\tau} a_{j_\tau, m_\tau}$$

and

$$H_{res} = -\tfrac{1}{2}\textstyle\sum_{L,M}(\kappa^L_0 + \kappa^L_1(\vec{\tau}_1 \cdot \vec{\tau}_2)) Q^\dagger_{LM}(1) Q_{LM}(2) - \\ -\tfrac{1}{2}\textstyle\sum_{L,J,M}(\kappa^{LJ}_0 + \kappa^{LJ}_1(\vec{\tau}_1 \cdot \vec{\tau}_2)) Q^\dagger_{LJM}(1) Q_{LJM}(2) .$$

Residual interaction Hamiltonian consists of two parts — the isoscalar and the isovector ones. It's convenient to write down scalar product of isospin Pauli matrices in the isovector part of residual interaction as

$$(\vec{\tau}_1 \cdot \vec{\tau}_2) = 4 t^0_1 t^0_2 + t^-_1 t^+_2 + t^+_1 t^-_2 .$$

Afterwards, the single particle operators of residual interaction can be written as follows

$$Q_{LM} = \sum_{j'm't'_3, jmt_3} < j'm't'_3 | f_L Y_{LM} \tau^k | jmt_3 > a^\dagger_{j'm't'_3} a_{jmt_3}$$

and

$$Q_{LJM} = \sum_{j'mt'_3, jmt_3} < j'm't'_3 | f_{LJ} [Y_L \sigma]_{JM} \tau^k | jmt_3 > a^\dagger_{j'm't'_3} a_{jmt_3} ,$$

where τ^k is the set of isospin operators $\hat{1}$, t^0, t^+, and t^-; $f_L(r)$ and $f_{LJ}(r)$ are the radial form factors of residual interaction operators. We will use, as in [6],

$$f_L(r) = f_{LJ}(r) = \frac{d}{dr} W(r) ,$$

where $W(r)$ is the central part of single-particle shell potential.

The terms containing the product of lowering and rising isospin operators $t_1^- t_2^+$ led to the particle-hole excitations which changes the charge of the nucleus and can be used to describe β-decay, μ-capture, (p,n)- and (n,p)-reactions. Correspondingly one can tell about the charge-exchange part of residual interaction which is the sum of products of operators like

$$\Omega_{JM} = \sum_{j_n m_n, j_p m_p} < j_n m_n | O_{JM} t^+ | j_p m_p > a^\dagger_{j_n,m_n} a_{j_p,m_p} ,$$

and Hermite conjugated to them. Here O_{JM} is multipole $/f_J(r)Y_J(\hat{\vec{r}})/$ or spin-multipole $/f_{LJ}(r)[Y_L(\hat{\vec{r}})\sigma]_J/$ operator.

The diagonalization of nuclear model Hamiltonian is done in two steps. At first step the Bogoliubov transformation taking into account pairing correlations of superconducting type is fulfilled for protons and neutrons independently

$$a_{j_\tau m_\tau} = u_{j_\tau} \alpha_{j_\tau m_\tau} + (-1)^{j_\tau - m_\tau} v_{j_\tau} \alpha^\dagger_{j_\tau, -m_\tau} .$$

Variational procedure

$$\delta \langle 0| \, H_0(\tau) - \lambda_\tau N_\tau - \sum_{j_\tau} \rho_{j_\tau} (u^2_{j_\tau} + v^2_{j_\tau} - 1) \, |0\rangle = 0$$

gives us u, v-coefficients and allows us to pas to the independent quasiparticles Hamiltonian:

$$H_0(\tau) \to \sum_{j_\tau m_\tau} \epsilon_{j_\tau} \alpha^\dagger_{j_\tau m_\tau} \alpha_{j_\tau m_\tau} ,$$

where $\epsilon_{j_\tau} = \sqrt{(E_{j_\tau} - \lambda_\tau)^2 + C_\tau^2}$ and $C_\tau = G_\tau \sum_{j_\tau} (j + 1/2)\, u_{j_\tau} v_{j_\tau}$. Averaging was done over quasiparticle vacuum state: $\alpha_{j_\tau m_\tau}|0> = 0$, which represents the ground state of the system of even nucleons number.

At the second step the interaction between two-quasiparticle states is taken into account. From the products of two quasiparticle operators the phonon operators are formed:

$$\Omega^i_{JM} = \sum_{j_p, j_n} \{ \psi^i_{j_p,j_n} [\alpha_{j_p}, \alpha j_n]_{J,M} - (-1)^{J-M} \phi^i_{j_p,j_n} [\alpha_{j_p}, \alpha_{j_n}]^\dagger_{J,-M} \} ,$$

where $[\alpha_{j_p}, \alpha_{j_n}]_{J,M} = \sum_{m_p,m_n} < j_p m_p j_n m_n | JM > \alpha_{j_p,m_p} \cdot \alpha_{j_n,m_n}$ and $< j_p m_p j_n m_n | JM >$ is the Clebsch-Gordan coefficient. In the random phase approximation phonon operators are supposed to obey to boson commutation rules. As the result the normalization and orthogonality conditions of one-phonon state are

$$\Phi(i,i') = \sum_{j_p,j_n} \{ \psi^i_{j_p,j_n} \psi^{i'}_{j_p,j_n} - \phi^i_{j_p,j_n} \phi^{i'}_{j_p,j_n} \} - \delta_{i,i'} = 0 .$$

The phonon amplitudes and the excitation energies of the one-phonon states are defined by the variational principle

$$\delta \{ < |\Omega^i_{JM} H_M \Omega^{i\dagger}_{JM}| > - < |H_M| > - \omega_i \Phi(i,i) \} = 0 ,$$

where $|>$ is the phonon vacuum state: $\Omega^i_{JM}|> = 0$. It gives the homogeneous system of linear equations:

$$\begin{aligned} R^+_{q,q'} g^i_{q'} - \omega_i w^i_q &= 0 \\ -\omega_i g^i_q + R^-_{q,q'} w^i_{q'} &= 0 , \end{aligned}$$

where

$$g^i_q = \psi^i_{j_p,j_n} + \phi^i_{j_p,j_n} , \quad w^i_q = \psi^i_{j_p,j_n} - \phi^i_{j_p,j_n} ,$$

$$R^\pm_{q,q'} = \epsilon_q \delta_{q,q'} - \frac{2\kappa^{J(LJ)}}{2J+1} h_q h_{q'} u^\pm_q u^\pm_{q'} ,$$

$$\epsilon_q = \epsilon_{j_p} + \epsilon_{j_n} , \quad u^\pm_q = u_{j_p} v_{j_n} \pm v_{j_p} u_{j_n} ,$$

$$h_q = < j_p || O_J t^- || j_n > .$$

The amplitudes of the transitions from the even-even ground state to the excited states with total spin J, its projection M and energy ω_i are equal to

$$b^+_{JM}(i) = \frac{1}{\sqrt{2J+1}} \sum_{j_p,j_n} < j_p || O_J t^- || j_n > (v_{j_p} u_{j_n} \psi^i_{j_p,j_n} + u_{j_p} v_{j_n} \phi^i_{j_p,j_n})$$

if the charge of the nucleus is decreased by unit, as in(n,p) reaction, or to

$$b^-_{JM}(i) = \frac{1}{\sqrt{2J+1}} \sum_{j_p,j_n} < j_p || O_J t^- || j_n > (u_{j_p} v_{j_n} \psi^i_{j_p,j_n} + v_{j_p} u_{j_n} \phi^i_{j_p,j_n})$$

if the charge is increased during transition as in (p,n) reaction. The transition strength is equal to $B^{\pm}_J(i) \equiv \sum_{M=-J}^{J} |b^{\pm}_{JM}(i)|^2$.

The parameters of the single particle potentials and of monopole pairing were fixed earlier. Only the effective constants of isovector residual interaction κ_1^L or κ_1^{LJ} were varied in our calculations.

The ordinary muon capture proceeds mainly through the spin-multipole transitions. The most important of them are the Gamow-Teller transitions ($\sigma t^{\pm}$ one-body operator) and the spin-dipole ($f(r)[Y_1,\sigma]_J t^{\pm}$ one-body operator) transitions. In this section we present the results of calculations of transition strength distribution over the excitation energy (strength function) for GT and spin-dipole transitions and compare them with the distributions extracted from (p,n) and (n,p) direct nuclear reactions at intermediate energies. The main goal of this section is to define the effective constants of residual interaction making comparison of calculated strength functions to those obtained from the experimental data, and afterwards to calculate the muon capture rates using these values for effective constants.

The theoretical and experimental results are shown in Figures 1–4 as the "running sums":

$$S^{\pm}(E) = \sum_{f:\ E_f - E_i \le E} \left| < f|\hat{O}t^{\pm}|i > \right|^2 .$$

By this sums one can show simultaneously the results of calculation which are set of discrete eigenvalues with corresponding transition strength and the experimental data which are often continuous function, especially if some strength is extracted from background. The fast variations in $S^{\pm}(E)$ indicate the presence of strong transitions in the energy regions where these variations occurs.

The results for the σt^- transition strength on ^{58}Ni are shown in Fig. 1. The excitation energies are reckoned from the ground state of the target nucleus every time. The experimental data, extracted from $^{58}Ni(p,n)^{58}Cu$ reaction at the forward angles (zero momentum transfer), are taken from the paper [7]. Lines "a" and "b" are the lower and upper limits of $S^-(E)$ obtained experimentally. The data from

Table 3 of [7] were used. Other curves represent the calculated values of $S^-(E)$. The line marked by "c" shows the strength function $S^-(E)$ obtained with the effective constants $\kappa_1^{01} = \kappa_1^{21} = -0.23/A$, "d" is for $S^-(E)$ calculated with $\kappa_1^{01} = \kappa_1^{21} = -0.43/A$, and "e" — for $\kappa_1^{01} = \kappa_1^{21} = -0.63/A$. The calculations with $\kappa_1^{01} = \kappa_1^{21} = -0.43/A$ give the correct position of GT resonance and describe reasonably distribution of the transition strength at the low excitation energy. But the total transition strength below $25\,MeV$ is larger than the experimentally observed one. The strength function calculated with $\kappa_1^{01} = -0.23/A$ has too much strength compared to the experimental data at the lowest excitation energies, it gives wrong position for the GT resonance and exceeds considerably observed total strength. The strength distribution marked by "e" is close to the "d" at the low excitation energies, but the energy position of the resonance is higher than the measured one and too much strength is shifted to the higher excitation energies. From this consideration one can conclude that the strength function calculated with the set of parameters $\kappa_1^{01} = \kappa_1^{21} = -0.43/A$ gives the better description of the experimentally obtained strength function $S^-(E)$ than other versions.

The running sums for the σt^+ strength functions for the ^{58}Ni are shown in Fig. 2. The legend and the values of effective constants of residual interactions are the same as in Fig. 1. The experiment in [8] shows, that practically all observed σt^+ transition strength in ^{58}Ni is concentrated in one wide bump, which is placed in the region of excitation energy between $3\,MeV$ and $8\,MeV$. In the calculations there is one collective state which contains the large fraction of the total transition strength. The position of this state depends on the κ_1^{01} value and it is located in the middle of the bump region at the $\kappa_1^{01} = \kappa_1^{21} = -0.43/A$ (line "d"). For all the effective constants used the calculated transition strength exceeds considerably the observed ones.

The theoretical value of the Gamow-Teller sum rule for ^{58}Ni is equal to

$$S^- - S^+ = 3(N - Z) = 6\,,$$

where $S^{\pm} \equiv S^{\pm}(\infty)$. In our calculations $S^- - S^+ = 5.26$ due to

nonorthogonality between neutron and proton single-particle wave functions. The experimentally defined sum rule value is $S^-(25) - S^+(25) = 3.7 \pm 2.2$ if one assumes that there is no σt^+ strength above the excitation energy of 10 MeV and there is no σt^- strength above 25 MeV. The calculated values are 3.81, 2.89 and 2.18 for the κ_1^{01} (and κ_1^{21}) equal to $-0.23/A$, $-0.43/A$ and $-0.63/A$ correspondingly. All calculated values fit into rather large interval of the experimental data. So the values $\kappa_1^{01} = \kappa_1^{21} = -0.43/A$ obtained from the σt^- strength function do not contradict to the data from σt^+ strength function on ^{58}Ni and to the measured value of Gamow-Teller transition strength.

The running sums for the Gamow-Teller t^- transition on the ^{60}Ni are shown in Fig. 3. The legend and used values of the effective constants of residual interaction are the same as in Fig. 1. The experimental data are taken from Table 4 and from Fig. 10 of [7]. The experimental strength function has one wide bump (its width is around 6 MeV) which sites between 10 and 20 MeV and contains more than 80% of total observed strength. The total observed strength is equal to 7.2 ± 1.8. The calculated strength functions have one collective transition too, but its position is higher than the experimental value. The calculated total transition strength is more than two times larger than the experimental one, but the strength located below 20 MeV is rather close to the one obtained from experiment.

The running sums of strength functions of σt^+ transitions on the ^{60}Ni are presented in Fig. 4. The experimental data are taken from Fig. 12 and Table II of [9]. The σt^+ transition strength located below 10 MeV is equal to 3.11 ± 0.08, but the total strength below 32 MeV is equal to 7.4 ± 0.5 [9]. This value should be compared to the value of total σt^- of 7.2 ± 1.8 obtained in [7]. The Gamow-Teller sum rules compiled from two experiments becomes -0.2 ± 2.2 but the theoretical value is $3(N - Z) = 12$. The calculated value of the total σt^+ transition strength decreases from 6.7 when κ_1^{01} and κ_1^{21} are equal to $-0.23/A$ to 4.6 at $\kappa_1^{01} = \kappa_1^{21} = -0.63/A$. The calculated value of the Gamow-Teller sum rule is 10.79 for all values of the effective constants of residual interactions. It means that either in [7] the σt^- strength is underestimated or in [9] the

σt^+ strength at higher excitation energies is overestimated significantly.

In order to fix the value of the effective constant of the spin-isospin residual interaction we have calculated the Gamow-Teller transition strength distribution over the excitation energy. The comparison of calculated strength function with the measured one leads to conclusion that the variant $\kappa_1^{01} = \kappa_1^{21} = -0.43/A$ gives the quite reasonable description of available experimental data concerning the Gamow-Teller transition strength in $^{58,60}Ni$.

Next problem to be solved is to fix the value of effective constant of spin-dipole–spin-dipole residual interactions. In order to do it the distributions of spin-dipole $(r[Y_1\sigma]_J t^-$, $J = 0, 1, 2)$ transition strength over the excitation energies were calculated for $^{58,60}Ni$. In the paper [7] there are few data concerning the distribution of $L = 1$ spin-isospin transition strength in $^{58,60}Ni$ measured in (p, n) reaction at intermediate energies. They give the outlook of the response function of $^{58,60}Ni$ to spin-isospin excitation due to the $L = 1$ angular moment transfer. The maxima of cross-section corresponding to the $L = 1$ transitions are located at ~ 26 MeV in ^{58}Ni and at ~ 25 MeV in ^{60}Ni (both energies are reckoned from the ground state of parent nucleus), and have estimated FWHM's of distributions equal to ~ 10 MeV and to ~ 12 MeV correspondingly. We have calculated the strength functions of spin-isospin $L = 1$ transition by summing the theoretical strength functions of spin-dipole transitions to the $J^\pi = 0^-$, $J^\pi = 1^-$ and $J^\pi = 2^-$ states. The results are shown in Tables 1 and 2. It can be seen from Tables that the spin-dipole–spin-dipole residual interactions with the effective constant equal to the $-0.33/A$ gives the reasonable agreement between calculated main characteristics (position of the resonance maxima and widths) and the observed ones.

Because there are no available experimental data concerning $Y_1 t^+$ transition strength we have checked the sensitivity of the calculated OMC rates to the variation of effective constant of isovector dipole residual interaction. The transitions from 0^+ ground states to the 1^- excited states have been considered, because only they are influenced by isovector dipole residual interactions within the RPA framework.

From Table 3 one can see that calculated OMC rate from the 0^+ ground state to the 1^- excited states is more sensitive to the variation of the effective constant of the spin-dipole residual interaction (κ_1^{11}) rather than to the changing of the effective constant of pure dipole interaction (κ_1^1). When the $|\kappa_1^1|$ increases more than by two times the OMC rate summed over all 1^- states reduces less than 10%. It can be easily seen from Table 3 that the OMC rate depends on the total spin-dipole transition strength mainly. The reduction of the OMC rate in two times corresponds to the decreasing of the total spin-dipole strength when κ_1^{11} varies from zero to $-0.43/A$. As a result, the isovector spin-dipole strength function is more important for the OMC rates than the dipole one. The same conclusion can be derived from the data of Table 4 in the ^{60}Ni case. From these Tables one can see that the OMC rate is rather weak influenced by the isovector dipole residual interaction. In considered cases the muon capture goes through the isovector spin-multipole transitions mainly. It was also noticed in [10].

Total OMC rates on $^{58,60,62}Ni$

After the set of effective constant of nuclear residual interaction is fixed we can use the eigenfunctions of nuclear model Hamiltonian for the calculation of the muon capture rates.

At the beginning we list the approximations which were done during the OMC and RMC rates calculations. The pseudoscalar coupling constant is defined by the expression

$$g_P(q^2) = \frac{m_\pi^2 + m_\mu^2}{m_\pi^2 + q^2}(\frac{g_P}{g_A})g_A(q^2)\,,$$

where $q^2 = (p-n)^2$ is the square of four-momentum transferred to the nucleons during muon capture. Velocity dependent terms were omitted during the calculations of both processes OMC and RMC. All muon capture rates are obtained with the following values of the constants of residual interaction — $\kappa_1^J = -0.103/A$, $\kappa_1^{LJ} = -0.33/A$, except $\kappa_1^{01} = \kappa_1^{21} = -0.43/A$.

The results of calculations of the OMC and RMC rates for nickel isotopes are presented in Tables 5–7 for several values of ratio g_P/g_A. The measured OMC rates are $(61.10 \pm 1.05)\ s^{-1}$ for ^{58}Ni, $(55.62 \pm 0.97)\ s^{-1}$ for ^{60}Ni and $(47.16 \pm 0.95)\ s^{-1}$ for ^{62}Ni from [11] and $(61.1 \pm 1.0)\ s^{-1}$ for ^{58}Ni, $(55.6 \pm 1.0)\ s^{-1}$ for ^{60}Ni and $(47.2 \pm 1.0)\ s^{-1}$ for ^{62}Ni from [12]. Both experiments give practically the same results for the total OMC rates on nickel isotopes. It can be easily seen from Tables 5 – 7 that the calculated total OMC rates for all used values of g_P/g_A are less than the measured one. Probably, the inclusion of velocity dependent terms may bring the calculated rates into better agreement with the experimental value. The calculations of [13] and the estimations of [14] shows that the velocity dependent terms increase the OMC rate by 10% at least. Our results are rather closed to the total muon capture rates calculated in finite Fermi system theory by Bunatyan [15] and are little less than the ones of [10]. It should be mentioned that contribution of transition into 1^- states of residual nuclei in our calculation are 4% less than in [10], but we have the relative weight of transitions into 1^+ states by 8% more than obtained in [10]. But in general our results concerning total OMC rates are in reasonable agreement with the experimental data and the results of previous calculations.

Total RMC rates on $^{58,60,62}Ni$

The results of total RMC rates and photon spectra are presented in Tables 8 and 9 and in Figs. 5–8. Fig. 5 shows the photon spectra calculated for different values of ratio g_P/g_A. The nuclear RMC amplitude was taken in the modified impulse approximation. The dependence of the calculated photon spectra from the g_P value will be seen more clear if one consider the photon spectra normalized by the calculated total OMC rate. Fig. 6 presents these normalized spectra. The theoretical photon spectra depend strongly on approximation which the RMC amplitude on nucleus is calculated. The differences in photon spectra are easily seen from Fig. 7. The total RMC rate on ^{58}Ni and its distribution over the states with definite total spin and parity are given in Table 8.

The main contributions into the total RMC rate in IA and MIA comes from the transition to the $1^{\pm}$ and 2^{-} states of daughter nucleus. But the rates corresponding to these transitions are reduced in MIA stronger as compared to IA. The most of strong suppression is for the rates to the 1^{+} excited states. At the large values of g_P/g_A the RMC rate corresponding to the transition to the 1^{+} excited states almost by six times less in MIA than in IA. The similar large difference in rates exist in the RMC on ^{60}Ni and ^{62}Ni too (see Table 9). The photon spectra calculated in MIA for three nickel isotopes are shown in Fig. 8.

Large difference in RMC rates obtained in MIA and IA requires certainly the deeper investigation of the physical nature of the modifications made in RMC amplitude due to the continuity-equation constraints [3].

Conclusion

For the first time the photon spectra and total radiative muon capture rate are calculated based on the microscopic description of nuclear response for heavy nuclei. Quasiparticle random phase approximation is used for the calculation of excitation spectra and transition amplitudes for the ordinary and radiative muon capture on $^{58,60,62}Ni$. The choice of the effective parameters of nuclear spin-isospin residual interactions is discussed. For that purpose the sum rule for the Gamow-Teller transitions is considered in connection with the total Gamow-Teller strength extracted from the $^{60}Ni(p,n)^{60}Cu$ [7] and $^{60}Ni(n,p)^{60}Co$ [9] experiments and it is assumed that in the last experiments the total σt^{+} transition strength is overestimated.

The calculated total rates of OMC on $^{58,60,62}Ni$ are close to the experimental data.

For the nuclear amplitude of radiative muon capture, besides the usual impulse approximation, the modified impulse approximation, in which the continuity equation for electric current is taken into account, is used. The results of calculations performed in both of approximations show that the inclusion of the continuity-equation constraint into RMC amplitude in nucleus reduces the RMC rate about two times. These corrections appeared to be stronger in the transitions from the 0^{+} ground state into $1^{\pm}$ excited states.

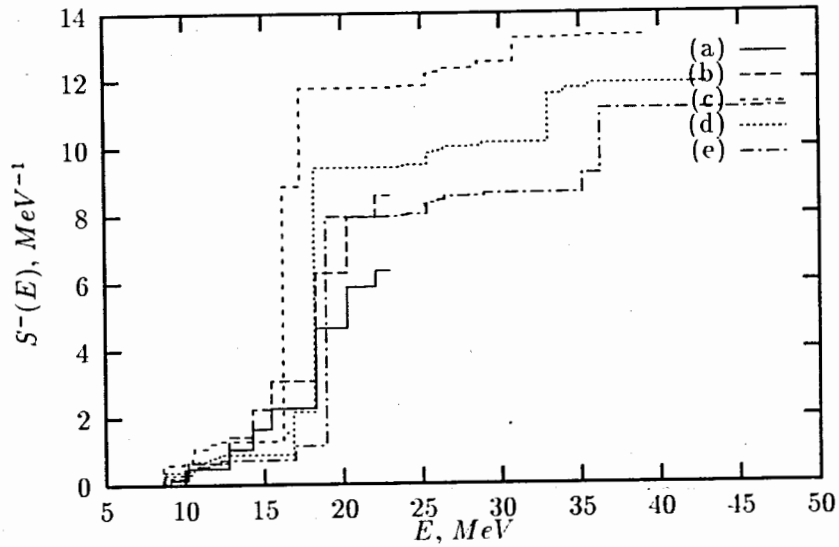

Figure 1: σt^{-} strength in ^{58}Ni

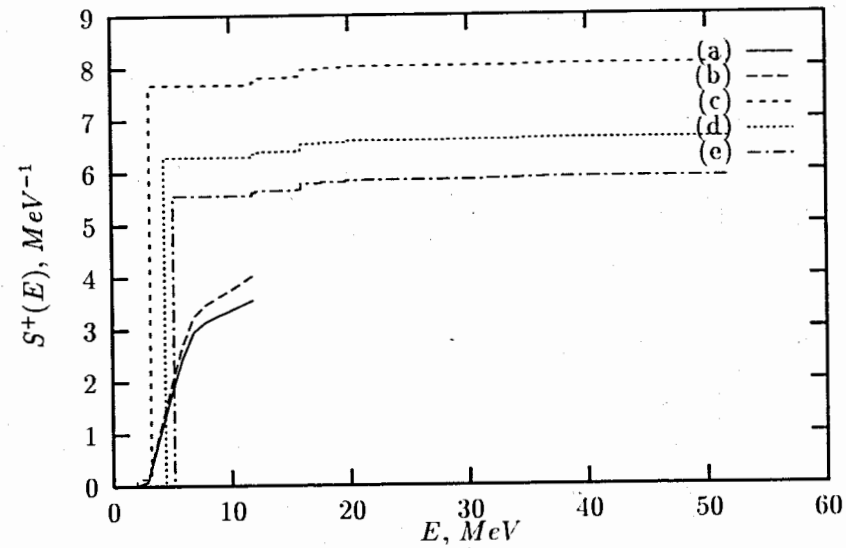

Figure 2: σt^{+} strength in ^{58}Ni

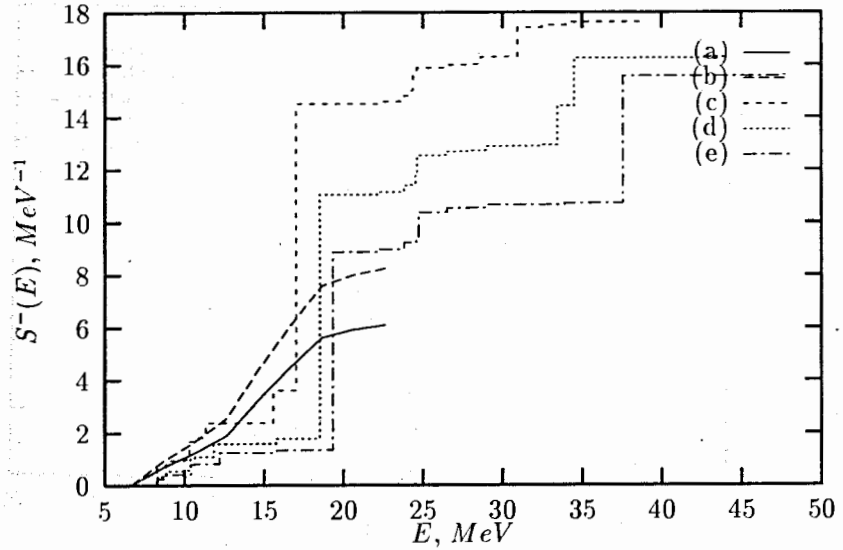

Figure 3: σt^- strength in ^{60}Ni

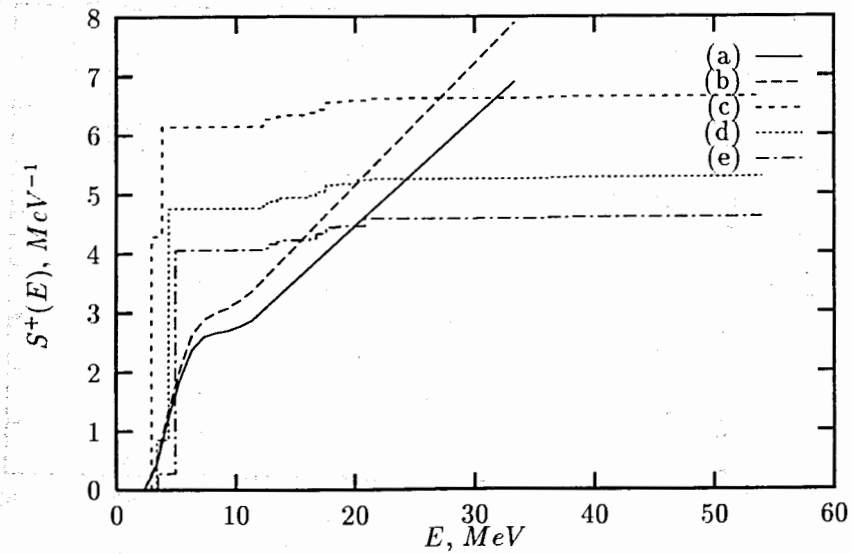

Figure 4: σt^+ strength in ^{60}Ni

Table 1: The main characteristics of the distribution of the spin-isospin dipole t^- transition strength in ^{58}Ni.

$\kappa_1^{1J} \cdot A$	Full $rY_1\sigma t^-$ strength (fm^2)	Energy centroid (MeV)	Dispersion (MeV)	Maximum localization (MeV)	Strength in maximum (fm^2)
-0.18	1111	27	4.1	29-30	370
-0.23	1050	29	5.0	31-32	346
-0.28	1000	30	5.4	32-33	298
-0.33	958	31	5.7	28-29	219
				33-34	227
-0.38	922	32	6.0	29-30	221
-0.43	891	34	6.4	30-31	215
				39-40	205

Table 2: The main characteristics of the distribution of the spin-isospin dipole t^- transition strength in ^{60}Ni.

$\kappa_1^{1J} \cdot A$	Full $rY_1\sigma t^-$ strength (fm^2)	Energy centroid (MeV)	Dispersion (MeV)	Maximum localization (MeV)	Strength in maximum (fm^2)
-0.18	1242	27	4.9	29-30	399
-0.23	1183	29	5.2	31-32	370
-0.28	1134	30	5.5	32-33	323
-0.33	1093	32	5.8	29-30	257
				33-34	235
-0.38	1057	33	6.1	29-30	254
				38-39	187
-0.43	1027	34	6.4	30-31	235
				39-40	240

Table 3: Dipole, spin-dipole transition strength and OMC rates in ^{58}Ni.

$\kappa_1^1 \cdot A$	$\kappa_1^{11} \cdot A$	Total OMC rate, s^{-1}	Total rY_1t^+ strength, fm^2	Total $r[Y_1\sigma]_1t^+$ strength, fm^2	Dipole strength res. reg., MeV	rY_1t^+ strength in res. reg., fm^2
−0.083	0.00	$37.7 \cdot 10^5$	314.8	558.8	6.1 – 11.4	239
−0.103	0.00	$37.3 \cdot 10^5$	298.4	559.2	6.1 – 11.5	240
−0.123	0.00	$37.0 \cdot 10^5$	284.0	559.6	6.1 – 11.5	238
−0.143	0.00	$36.6 \cdot 10^5$	271.3	559.9	6.1 – 11.6	234
−0.203	0.00	$35.9 \cdot 10^5$	240.7	560.8	6.1 – 12.0	219
−0.083	−0.23	$23.5 \cdot 10^5$	317.5	322.0	6.2 – 11.4	221
−0.103	−0.23	$23.1 \cdot 10^5$	300.8	322.1	6.2 – 11.4	232
−0.123	−0.23	$22.7 \cdot 10^5$	286.3	322.2	6.2 – 11.4	234
−0.143	−0.23	$22.3 \cdot 10^5$	273.4	322.3	6.2 – 11.5	232
−0.203	−0.23	$21.5 \cdot 10^5$	242.4	322.6	6.2 – 11.7	217
−0.083	−0.33	$21.1 \cdot 10^5$	318.2	281.5	6.2 – 11.4	226
−0.103	−0.33	$20.7 \cdot 10^5$	301.4	281.6	6.2 – 11.4	237
−0.123	−0.33	$20.3 \cdot 10^5$	286.8	281.7	6.2 – 11.4	239
−0.143	−0.33	$19.9 \cdot 10^5$	273.9	281.8	6.2 – 11.5	236
−0.203	−0.33	$19.1 \cdot 10^5$	242.9	282.0	6.2 – 11.7	221
−0.083	−0.43	$19.4 \cdot 10^5$	318.7	252.6	6.2 – 11.4	229
−0.103	−0.43	$19.0 \cdot 10^5$	301.9	252.7	6.2 – 11.4	239
−0.123	−0.43	$18.6 \cdot 10^5$	287.3	252.7	6.2 – 11.4	241
−0.143	−0.43	$18.3 \cdot 10^5$	274.4	252.8	6.2 – 11.5	238
−0.203	−0.43	$17.4 \cdot 10^5$	243.3	253.0	6.3 – 11.7	222

Table 4: Dipole, spin-dipole transition strength and OMC rates in ^{60}Ni

$\kappa_1^1 \cdot A$	$\kappa_1^{11} \cdot A$	Total OMC rate, s^{-1}	Total rY_1t^+ strength, fm^2	Total $r[Y_1\sigma]_1t^+$ strength, fm^2	Dipole strength res. reg., MeV	rY_1t^+ strength in res. reg., fm^2
−0.083	0.00	$35.2 \cdot 10^5$	289.9	525.9	6.3 – 11.9	200
−0.103	0.00	$34.8 \cdot 10^5$	273.9	526.3	6.3 – 11.9	200
−0.123	0.00	$34.4 \cdot 10^5$	260.0	526.7	6.3 – 11.9	198
−0.143	0.00	$34.1 \cdot 10^5$	247.6	527.0	6.3 – 11.9	193
−0.203	0.00	$33.4 \cdot 10^5$	217.8	528.0	6.3 – 12.0	171
−0.083	−0.23	$21.9 \cdot 10^5$	292.8	300.4	6.3 – 13.0	190
−0.103	−0.23	$21.5 \cdot 10^5$	276.6	300.5	6.3 – 11.9	190
−0.123	−0.23	$21.2 \cdot 10^5$	262.5	300.7	6.0 – 11.9	205
−0.143	−0.23	$20.8 \cdot 10^5$	250.0	300.8	6.0 – 11.9	201
−0.203	−0.23	$20.1 \cdot 10^5$	219.7	301.2	6.0 – 11.9	178
−0.083	−0.33	$19.7 \cdot 10^5$	293.5	260.8	6.3 – 13.0	194
−0.103	−0.33	$19.3 \cdot 10^5$	277.3	260.9	6.0 – 11.9	211
−0.123	−0.33	$18.9 \cdot 10^5$	263.1	261.0	6.0 – 11.9	210
−0.143	−0.33	$18.6 \cdot 10^5$	250.6	261.1	6.0 – 11.9	205
−0.203	−0.33	$17.8 \cdot 10^5$	220.2	261.4	6.1 – 12.0	181
−0.083	−0.43	$18.1 \cdot 10^5$	294.1	232.4	6.0 – 13.0	219
−0.103	−0.43	$17.7 \cdot 10^5$	277.9	232.5	6.0 – 11.9	215
−0.123	−0.43	$17.3 \cdot 10^5$	263.6	232.5	6.0 – 11.9	213
−0.143	−0.43	$17.0 \cdot 10^5$	251.1	232.6	6.1 – 11.9	208
−0.203	−0.43	$16.2 \cdot 10^5$	220.6	232.9	6.1 – 12.0	183

Table 5: Total OMC rates and relative contribution (in percent) into it from the states with definite spin and parity on ^{58}Ni.

g_P/g_A	Tot. OMC rate, s^{-1}	J^π							
		0^+	0^-	1^+	1^-	2^+	2^-	3^+	3^-
4.0	$60.4 \cdot 10^5$	2.5	4.0	26.6	34.2	9.3	16.8	5.3	1.3
6.0	$58.1 \cdot 10^5$	2.6	3.2	26.1	35.6	9.6	16.4	5.1	1.3
8.0	$56.0 \cdot 10^5$	2.7	2.4	25.5	36.9	10.0	16.1	5.0	1.4
10.0	$54.4 \cdot 10^5$	2.8	1.7	25.1	38.0	10.3	15.8	4.9	1.4
12.0	$53.0 \cdot 10^5$	2.9	1.1	24.7	39.0	10.6	15.5	4.8	1.4

Table 6: Total OMC rates and relative contribution (in percent) into it from the states with definite spin and parity on ^{60}Ni.

g_P/g_A	Tot. OMC rate, s^{-1}	J^π							
		0^+	0^-	1^+	1^-	2^+	2^-	3^+	3^-
4.0	$54.9 \cdot 10^5$	2.7	4.2	25.7	35.1	9.6	16.0	5.4	1.3
6.0	$52.8 \cdot 10^5$	2.8	3.4	25.2	36.5	10.0	15.6	5.2	1.4
8.0	$51.0 \cdot 10^5$	2.9	2.6	24.7	37.8	10.3	15.3	5.1	1.4
10.0	$49.5 \cdot 10^5$	3.0	1.8	24.2	38.9	10.6	15.0	4.9	1.5
12.0	$48.2 \cdot 10^5$	3.1	1.2	23.8	39.9	10.9	14.7	4.8	1.5

Table 7: Total OMC rates and relative contribution (in percent) into it from the states with definite spin and parity on ^{62}Ni.

g_P/g_A	Tot. OMC rate, s^{-1}	J^π							
		0^+	0^-	1^+	1^-	2^+	2^-	3^+	3^-
4.0	$49.6 \cdot 10^5$	2.9	4.4	25.5	35.4	9.9	15.1	5.5	1.4
6.0	$47.7 \cdot 10^5$	3.1	3.5	24.9	36.8	10.3	14.7	5.3	1.4
8.0	$46.1 \cdot 10^5$	3.2	2.6	24.4	38.1	10.6	14.4	5.2	1.5
10.0	$44.7 \cdot 10^5$	3.3	1.9	24.0	39.2	11.0	14.1	5.0	1.5
12.0	$43.6 \cdot 10^5$	3.3	1.2	23.6	40.2	11.2	13.9	4.9	1.6

Table 8: Total and partial RMC rates on ^{58}Ni calculated in two approximations for the radiative muon capture amplitude on nucleus.

g_P/g_A	Appr.	RMC rate, s^{-1}								
		total	0^+	0^-	1^+	1^-	2^+	2^-	3^+	3^-
4.0	IA	250.1	5.2	7.4	127.6	60.6	8.9	34.4	5.4	0.6
	MIA	133.5	2.7	3.4	52.0	41.2	7.3	22.4	4.0	0.5
6.0	IA	286.3	5.2	7.7	149.8	66.5	9.6	40.5	6.3	0.6
	MIA	133.6	2.7	3.1	48.6	43.9	7.8	23.0	4.1	0.5
8.0	IA	331.3	5.1	8.1	176.9	74.1	10.7	48.2	7.5	0.6
	MIA	135.5	2.7	2.6	45.8	47.0	8.4	24.0	4.3	0.5
10.0	IA	385.0	5.1	8.5	209.0	83.4	11.9	57.5	8.9	0.7
	MIA	139.1	2.7	2.3	43.5	50.7	9.2	25.5	4.6	0.5
12.0	IA	447.5	5.0	9.1	246.1	94.4	13.4	68.3	10.6	0.7
	MIA	144.4	2.7	2.0	41.8	54.9	10.0	27.5	4.9	0.6

Table 9: Total RMC rates on $^{58,60,62}Ni$ calculated in two approximations for nuclear RMC amplitude for different values of g_P/g_A.

Nucleus	Approx.	RMC rates, s^{-1}				
		4.0	6.0	8.0	10.0	12.0
^{58}Ni	IA	250.1	286.3	331.3	385.0	447.5
	MIA	133.5	133.6	135.5	139.1	144.4
^{60}Ni	IA	215.6	246.5	284.9	330.8	384.3
	MIA	117.0	117.5	119.7	123.4	128.6
^{62}Ni	IA	184.0	210.1	242.7	281.6	327.1
	MIA	101.3	102.2	104.4	108.1	113.1

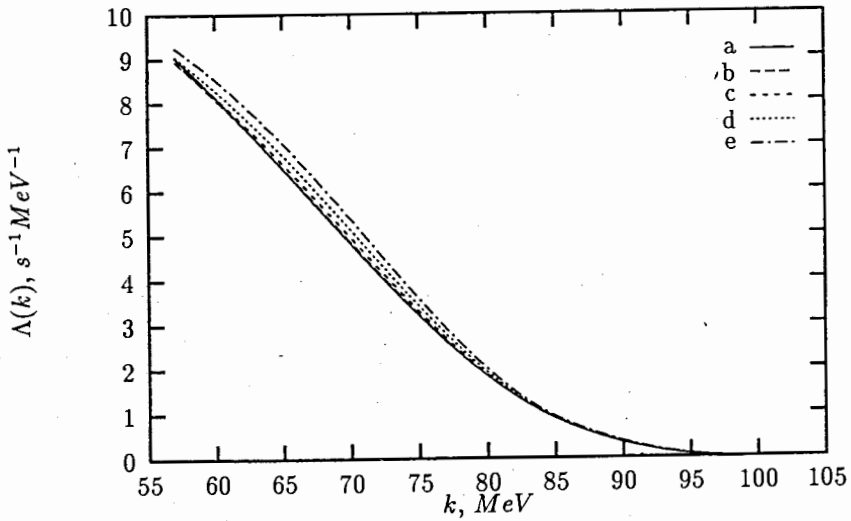

Figure 5: Photon spectra from RMC on ^{58}Ni calculated for ratio g_P/g_A equal to 4.0 (curve a), 6.0 (curve b), 8.0 (curve c), 10.0 (curve d) and 12.0 (curve e).

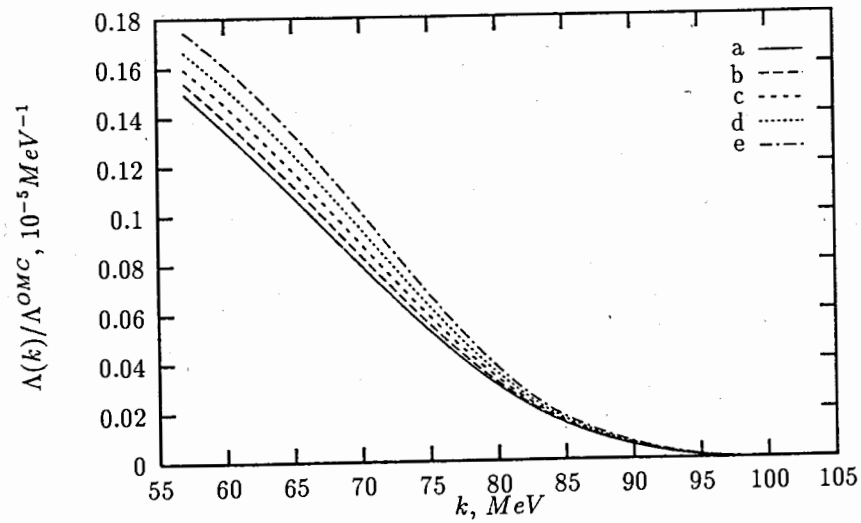

Figure 6: Calculated photon spectra from RMC on ^{58}Ni normalised by calculated total OMC rates. The curves labels are as for Fig. 5

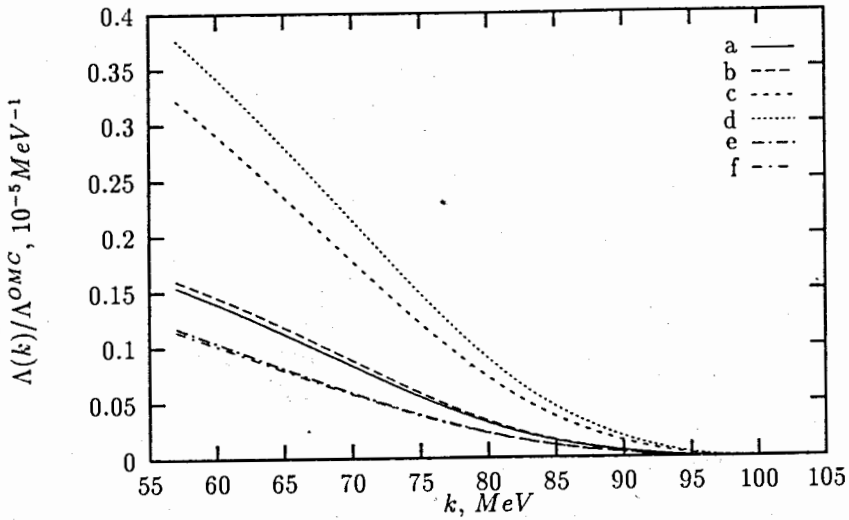

Figure 7: Photon spectra from RMC on ^{58}Ni calculated in three approximations for nuclear RMC amplitude: MIA (curves a and b), IA (c and d) and model case when only muon can radiate (e and f). The curves a, c and e are calculated with $g_P/g_A = 6.0$, other lines – with $g_P/g_A = 8.0$.

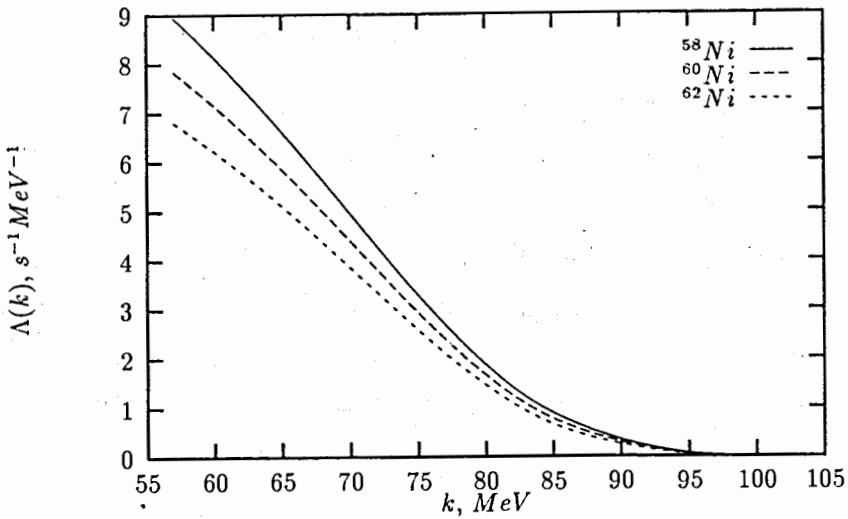

Figure 8: Photon spectra from RMC on $^{58,60,62}Ni$ calculated with $g_P/g_A = 8.0$.

We would like to thank T. Gorringe and K. Junker for many useful discussions. This work was supported in part by Russian Foundation for Basic Research (grant 95-02-04279) and by National Science Foundation (USA).

References

[1] H.P.C. Rood and H.A. Tolhoek, 1965, Nucl. Phys., **70**, 658

[2] K.W. Ford and J.G. Wills, 1962, Nucl. Phys., **35**, 295

[3] M. Gmitro, A.A. Ovchinnikova and T.V. Tetereva, 1986, Nucl. Phys., **A453**, 685

[4] G.E. Pustovalov, 1959, Sov. Phys. JETP, **36(9)**, 1288

[5] V.G. Soloviev, *Theory of complex nuclei*, 1976, Pergamon Press, Oxford a.o.

[6] A.I. Vdovin and V.G. Soloviev, Part. and Nucl., 1983, **14**, 99

[7] J. Rapaport *et al*, 1983, Nucl. Phys., **A410**, 371

[8] S. El-Kateb *et al*, 1994, Phys. Rev., **C49**, 3128

[9] A.L. Williams *et al*, 1995, Phys. Rev., **C51**, 1144

[10] O. Nalcioğlu, D.J. Rowe and C. Ngo-Trong, 1974, Nucl. Phys., **A218**, 495

[11] V.D. Bobrow *et al*, 1965, Sov. Phys. JETP, **21**, 799

[12] T. Suzuki, D.F. Measday and J.P. Roalsvig, 1987, Phys. Rev. **C35**, 2212

[13] N. Auerbach and A. Klein, 1984, Nucl. Phys., **A422**, 480

[14] M.G. Urin and O.N. Vyazankin, 1992, Nucl. Phys., **A537**, 534

[15] G.G. Bunatyan, 1966, Sov. J. Nucl. Phys., **3**, 613

Received by Publishing Department
on December 20, 1996.

Эрамжян Р.А., Кузьмин В.А., Тетерева Т.В. E4-96-478

Расчеты обычного и радиационного захвата мюонов ядрами ^{58,60,62}Ni

Впервые вычислены спектры фотонов и полная скорость радиационного захвата мюонов тяжелыми ядрами на основе микроскопического описания ядерной функции возбуждения. Для расчета спектров возбуждения и амплитуд переходов для обычного и радиационного захвата мюонов ядрами ^{58,60,62}Ni используется квазичастичное приближение случайных фаз. Обсуждается выбор эффективных параметров спин-изоспиновых остаточных взаимодействий. Для этого проведено сравнение вычисленных силовых функций гамов-теллеровских ($\sigma t^{\pm}$) и спин-дипольных ($r[Y_1\sigma]_{0,1,2}t^{-}$) переходов с экспериментальными данными. Обсуждается правило сумм для гамов-теллеровских переходов. При вычислении амплитуды радиационного захвата мюонов ядром кроме обычного импульсного приближения используется модифицированное импульсное приближение, в котором учитывается уравнение непрерывности для электромагнитного тока. Вычисленные полные скорости обычного захвата мюонов близки к значениям, полученным экспериментально.

Работа выполнена в Лаборатории теоретической физики им. Н.Н.Боголюбова ОИЯИ.

Препринт Объединенного института ядерных исследований. Дубна, 1996

Eramzhyan R.A., Kuz'min V.A., Tetereva T.V. E4-96-478

Calculations of the Ordinary and Radiative Muon Capture on ^{58,60,62}Ni

For the first time the photon spectra and total rate of radiative muon capture on heavy nuclei are calculated on the base of the microscopic description of nuclear excitation function. Quasiparticle random phase approximation is used for the calculation of excitation spectra and transition amplitudes for the ordinary and radiative muon capture on ^{58,60,62}Ni. The choice of the effective parameters of nuclear spin-isospin residual interactions is discussed. The strength functions of Gamov-Teller ($\sigma t^{\pm}$) and spin-dipole ($r[Y_1\sigma]_{0,1,2}t^{-}$) transitions are calculated and compared with the experimental data. The sum rule for Gamov-Teller transitions is considered too. For the nuclear amplitude of radiative muon capture, besides the usual impulse approximation, the modified impulse approximation, in which the continuity equation for electromagnetic current is taken into account, is used. The calculated total rates of ordinary muon capture are close to the experimental data.

The investigation has been performed at the Bogoliubov Laboratory of Theoretical Physics, JINR.

Preprint of the Joint Institute for Nuclear Research. Dubna, 1996